

# Functions of the SLC36 transporter Pathetic in growth control

Wen-Yang Lin, Claire R Williams, Connie Yan, and Jay Z Parrish\*

Department of Biology; University of Washington; Seattle, WA USA

**Keywords:** amino acid transporter, dendrite, drosophila, growth control, translation

Neurons exhibit extreme diversity in size, but whether large neurons have specialized mechanisms to support their growth is largely unknown. Recently, we identified the SLC36 transporter Pathetic (Path) as a factor required for extreme dendrite growth in neurons. Path is broadly expressed, but only neurons with large dendrite arbors or small neurons that are forced to grow large require *path* for their growth. To gain insight into the basis of growth control by *path*, we generated additional alleles of *path* and further examined the apparent specificity of growth defects in *path* mutants. Here, we confirm our prior finding that loss of *path* function imposes an upper limit on neuron growth, and additionally report that *path* likely limits overall neurite length rather than dendrite length alone. Using a GFP knock-in allele of *path*, we identify additional tissues where *path* likely functions in nutrient sensing and possibly growth control. Finally, we demonstrate that *path* regulates translational capacity in a cell type that does not normally require *path* for growth, suggesting that *path* may confer robustness on growth programs by buffering translational output. Altogether, these studies suggest that Path is a nutrient sensor with widespread function in *Drosophila*.

## Introduction

Neurons exhibit extreme diversity in size, but how growth programs are tailored to meet the respective demands of small and large neurons is largely unknown. From a genetic screen for mutations that differentially affected growth in *Drosophila* sensory neurons with different sized dendrite arbors, we identified *pathetic* (*path*) as a gene that selectively affects dendrite growth in neurons with large dendrite arbors.<sup>1</sup> In *path* mutants, dendrite growth arrests at a fixed upper limit of dendrite length in neurons that normally have differently sized arbors. While *path* is normally dispensable for growth in neurons with small dendrite arbors, forcing these neurons to elaborate complex dendrite arbors reveals that these neurons likewise require *path* for growth beyond the same upper limit of dendrite growth. Thus, *path* appears to define a pathway required to support extreme growth demands in neurons.

How does *path* modulate neuron growth? *path* encodes an SLC36 family transporter that paradoxically displays very low transport capacity under physiological conditions<sup>2,3</sup> leading to the model that Path functions similar to other transporter-related receptors (tranceptors) to regulate signaling in response to metabolites. Examples of tranceptors include the System A amino acid transporter SNAT2, which regulates transcription in response to amino acid binding<sup>4</sup> and GLUT2, a sugar transporter that has transport-independent functions as a receptor for extracellular

glucose.<sup>5</sup> With respect to growth control in neurons, Path regulates translational capacity,<sup>1</sup> but how Path couples nutrient status to translational control is unknown. One model that has been proposed is that Path functions as a nutrient sensor for the target of rapamycin complex 1 (TORC1).<sup>2</sup> In support of this model, one study demonstrated that SLC36A1 and Path can interact with components of the Ragulator complex,<sup>6</sup> which links amino acid availability to TORC1 activation.<sup>7</sup> However, other studies have yielded different results. For example, proteomic analysis of SLC36-interacting proteins failed to identify interactions between SLC36 transporters and Ragulator or TORC1 components,<sup>8</sup> and SLC36A1 overexpression antagonizes TORC1 activation in some contexts.<sup>9</sup> Furthermore, we found no evidence of interactions between Path and TORC1 in developmental control of neuron growth,<sup>1</sup> though gain-of-function experiments suggest that Path can promote neuron growth together with TORC1.

Several prominent questions remain regarding the function of Path and other SLC36 family transporters in growth control. First, the nature of interactions between Path and TORC1 and whether these interactions differ according to cell type or cellular state merits further study. Second, although Path is broadly expressed in neurons and non-neuronal cells, mutation of *path* affects growth in neurons with large dendrite arbors, but not in other cells. Whether this apparent specificity reflects cellular differences in Path function, regulation, or redundancy with other SLC36 transporters is unknown. Finally, the nature of the

\*Correspondence to: Jay Z Parrish; Email: jzp2@uw.edu

Submitted: 10/21/2015; Revised: 11/30/2015; Accepted: 12/02/2015

<http://dx.doi.org/10.1080/19336934.2015.1129089>

**Original Article:** Lin WY, Williams C, Luedke KA, Yan C, Ahn J, Morrison N, Bloomsburg S, Duncan K, Kim CK, Parrish JZ. Identification of an amino acid transporter required to support extreme growth in neurons. *Genes & Development* 2015; 29:1120-1135; PMID: PMC4470281; <http://dx.doi.org/10.1101/gad.259119.115>.

metabolites that elicit Path-dependent signaling *in vivo* remain elusive, though amino acids are the most likely candidates. As a first step to answering these questions, we generated new alleles of *path* that facilitate functional analysis of the gene product *in vivo*. Here, we provide additional support for the notion that *path* is required for growth above a fixed limit in neurons. Using a functional GFP knock-in allele of *path* we provide an overview of Path expression and localization in well-fed larvae, defining likely sites of Path function. Finally, we provide evidence that Path regulates translational output in non-neuronal cells.

## Results

### Path is required for dendrite growth beyond a fixed limit

We previously found that *path* is required for dendrite growth above a fixed limit in PNS neurons, but appears to be dispensable for growth of other larval tissues.<sup>1</sup> Our prior analyses made use of a nonsense mutation (*path<sup>dg50</sup>*) that behaved as a strong loss of function with regard to dendrite growth, however this allele retained coding sequences for the entire N-terminal intracellular

domain. We therefore set out to assay whether the truncated protein encoded by this allele provided residual activity for dendrite growth, animal viability or growth of other cell types. To this end, we used CRISPR-Cas9-mediated genome editing<sup>10,11</sup> to generate a deletion allele of *path* (*path<sup>Δ</sup>*) that removed the entire short isoform, leaving coding sequences for the first 16 amino acids of the long isoform of *path* but no other portion of the protein (Fig. 1A). Similar to *path<sup>dg50</sup>*, larvae homozygous for the *path<sup>Δ</sup>* allele were also viable and had no significant defects in overall larval growth (data not shown). Likewise, *path<sup>Δ</sup>* caused severe defects in C4da dendrite growth on its own or in combination with a chromosomal deficiency [*Df(3L)BSC773*; hereafter referred to as *Df*] that spans the entire *path* locus (Fig. 1C). Notably, dendrites of C4da neurons arrested at the same fixed value of total dendrite length in *path<sup>dg50/Df</sup>* and *path<sup>Δ/Df</sup>* mutant larvae (Fig. 1C), strongly suggesting that this represents a complete loss-of-function phenotype. Given that this allele of *path* is viable, it should be possible to use this allele for systematic analysis of *path* function in other contexts as well.

Whereas PNS neurons require *path* for extreme growth, *path* is dispensable for cell growth in body wall epithelial cells,

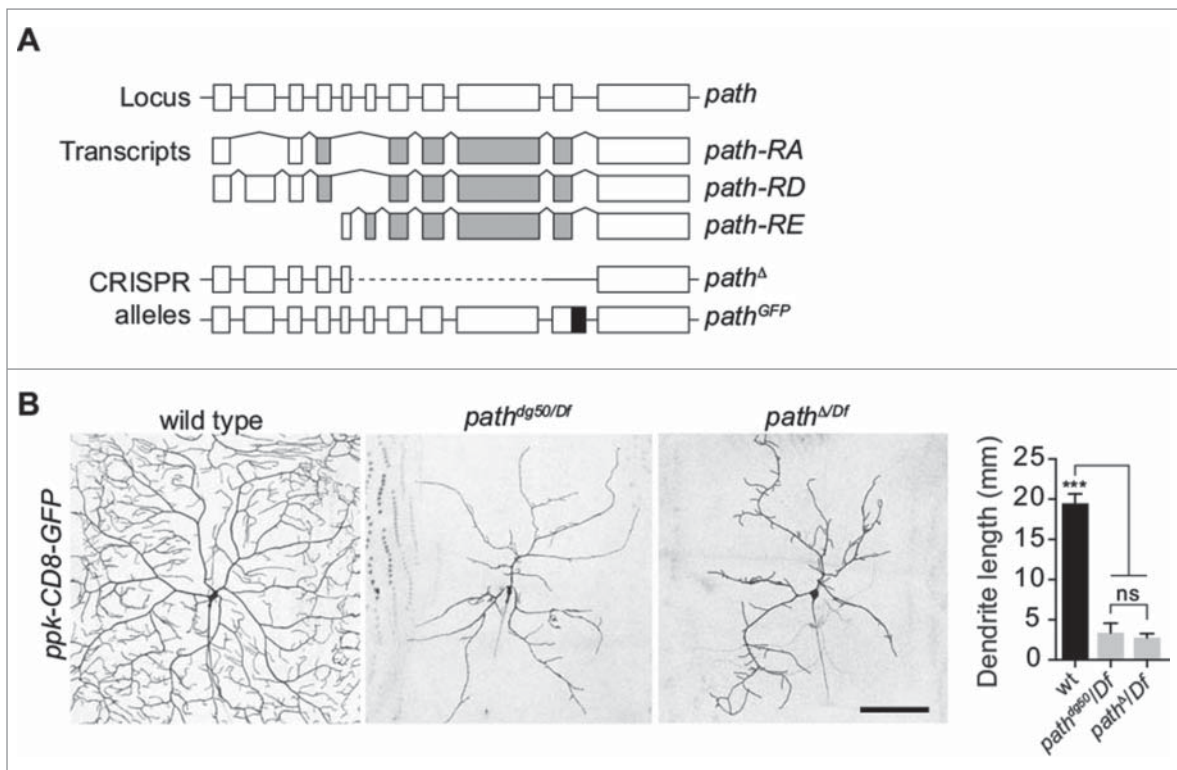


**Figure 1.** Generation of new *path* alleles. **(A)** Schematic of the *path* locus, *path* transcripts, and new alleles generated by CRISPR-based genome engineering. Lines depict introns and boxes depict exons (empty boxes, non-coding; shaded, protein coding). The *path* locus encodes three documented transcripts and two polypeptides with alternative 5' coding exons yielding different intracellular domains. The *path<sup>Δ</sup>* allele deletes the entire *path-RE* transcript including the four coding exons shared by all *path* transcripts and the *path<sup>GFP</sup>* allele contains GFP coding sequences fused in-frame upstream of the Path stop codon. **(B)** *path<sup>Δ</sup>* is a loss-of-function allele. Left, representative images C4da neurons in wild type or *path* mutant larvae. Right, quantification of dendrite length in the indicated genotypes ( $n > 6$  neurons for each genotype). Dendrite lengths of *path<sup>dg50/Df</sup>* and *path<sup>Δ/Df</sup>* mutants are significantly different from wild type controls (\*\*\*,  $< 0.001P$ ) but not significantly different from one another (ns), one-way analysis of variance (ANOVA) with Tukey's HSD *post hoc* analysis. Scale bar, 100  $\mu$ m. Genotypes: wt;  $w^{118}/ppk-CD8-GFP$ ; *path<sup>dg50/Df</sup>*;  $w^{118}/ppk-CD8-GFP$ ; *path<sup>dg50/Df(3L)BSC773</sup>*; *path<sup>Δ/Df</sup>*;  $w^{118}/ppk-CD8-GFP$ ; *path<sup>Δ/Df(3L)BSC773</sup>*.

oocytes, fat bodies, and salivary glands, as well as overall animal growth in larva and adult flies under well-fed laboratory conditions.<sup>1</sup> However, we cannot rule out a role for *path* in imparting robustness to growth programs, or modulating growth programs under stressful conditions (see below). In contrast to our observations, a prior study relying on a P-element insertion allele of *path* (*path*<sup>KG06640</sup>) reported that *path* influenced overall animal growth.<sup>2</sup> Although we found that *path*<sup>KG06640</sup> is a strong hypomorphic *path* allele, we observed no overt effects of *path* mutation on animal growth in any allelic combination<sup>1</sup>. Notably, our studies included *path*<sup>KG06640</sup> as well as 2 molecularly defined amorphic *path* alleles. We therefore speculate that second-site mutations may have contributed to the reported effects of *path*<sup>KG06640</sup> on animal growth. Alternatively, *path* function in animal growth could be responsive to nutrients that differed in the food sources in the prior study and our more recent studies. Nevertheless, we conclude that under well-fed conditions, *path* is dispensable for overall animal growth.

### Path regulates overall neuron size

Path localizes to both axons and dendrites, and our working model for *path* function in neuronal growth control is that Path regulates translational capacity of neurons. With this in mind, it's unclear how Path could selectively regulate dendrite growth. Our prior studies indicated that *path* is required for dendrite growth beyond a fixed limit; whether *path* similarly affects axon growth has not been investigated. We therefore wanted to determine whether *path* was responsive to growth demands of dendrites alone or axons and dendrites.

Axon outgrowth precedes dendrite development in *Drosophila* embryonic PNS neurons, with axons innervating targets in the ventral nerve cord (VNC) (Fig. 2A). Because the VNC is located anteriorly, larval sensory neurons in posterior segments have longer axons than corresponding neurons in anterior segments. If *path* is setting an upper limit on dendrite growth, as we previously hypothesized,<sup>1</sup> we would expect dendrites of C4da neurons

in different segments to arrest at the same fixed value of dendrite length. In contrast, if *path* is responsive to growth demands of axons and dendrites, dendrites in PNS neurons with longer axons should be more severely affected by loss of *path*. Our prior analysis of *path* function in dendrite growth involved PNS neurons located in a fixed position along the anterior-posterior (AP) axis,<sup>1</sup> which therefore had axons of the same length, so we examined whether C4da dendrite growth was more severely affected in PNS neurons located in posterior segments of *path* mutants (Fig. 2A). To this end, we measured dendrite length of C4da neurons in 3 abdominal segments (A2, A5, A8) and compared mean dendrite lengths of neurons in segment A2 to those in A5 and A8. We found that C4da neurons in posterior segments had significantly shorter dendrites and fewer dendritic branches in *path* mutant larvae (Fig. 2B–C), consistent with the notion that *path* mutation sets an upper limit on total neurite length rather than dendrite length alone.

We next assayed for growth defects in axons by visualizing terminal axonal arbors of C4da neurons. Whereas axonal arbors of *path* mutant C4da neurons were indistinguishable from controls prior to 48 h after egg laying (AEL), *path* mutant axonal arbors exhibited progressive growth defects that were more severe in posterior segments. By 120 h AEL, C4da neurons in posterior segments exhibited severe defects in axon growth (Fig. 2D). By contrast, we observed no effect on the overall axon length or terminal arbor of motor neurons that innervate dorsal muscles (data not shown), possibly because the total neurite length of motor axons and dendrites is below the threshold for *path*-dependent growth. We conclude that mutations in *path* likely impose an upper limit on overall neurite (axon and dendrite) growth, rather than setting an upper limit on dendrite length alone, and that *path* function is dispensable for growth below this limit.

### Path is differentially expressed in different larval tissues

One prominent model for SLC36 transporter function in growth control is that SLC36 transporters serve as nutrient

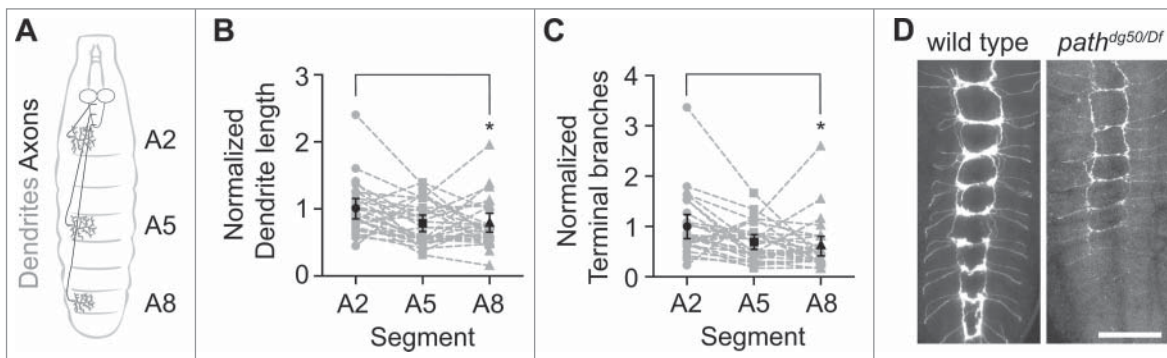


**Figure 2.** *path* imposes a limit on total neurite length. (A) Schematic depiction of axon (black) and dendrite (gray) arbors of C4da neurons in abdominal segments A2, A5, and A8. Sensory neurons in more posterior segments have longer axons. Plots depict relative C4da dendrite length (B) and branch number (C) in abdominal segments A2, A5, and A8 in each of 30 *path*<sup>dg50</sup>/*Df* larvae. Values are normalized to mean values for segment A2. Dashed lines connect data points derived from the same larva, black points mark the mean for each segment, and error bars represent the standard deviation. \* $<0.05P$ , two-way analysis of variance (ANOVA) with Tukey's HSD *post hoc* analysis. (D) Axonal arbors of C4da neurons in wt control or *path*<sup>dg50</sup>/*Df* mutant larvae. Anterior is up, scale bar is 50  $\mu$ m. Genotype: wt: *w*<sup>118</sup>; *ppk-CD4-tdTomato*; *path*<sup>dg50</sup>/*Df*: *w*<sup>118</sup>; *path*<sup>dg50</sup>, *ppk-CD4-tdTomato/DF(3L)BSC773*, *ppk-CD4-tdTomato*.

sensors for TORC1.<sup>12</sup> Two predictions of this model are that SLC36 transporters should be responsive to amino acids and that they should localize to lysosomes, where TORC1 is activated.<sup>9</sup> In support of the first prediction, some SLC36 transporters bind amino acids with a high degree of specificity,<sup>2,3,13,14</sup> though different SLC36 transporters show different binding preferences and markedly different transport properties. Confounding the potential link to TORC1, different SLC36 transporters appear to localize differently. Whereas SLC36A1 is most active at acidic pH and predominantly localizes to lysosomes,<sup>14</sup> Path and its closest vertebrate counterpart SLC36A4 are most active at neutral pH and appear to localize to the plasma membrane and a number of intracellular compartments.<sup>1,15</sup> However, analysis of SLC36 protein distribution has relied on antibody staining, which can be confounded by lack of antibody specificity, artifacts of fixation, and tracking of ectopically expressed epitope-tagged proteins, which may or may not reflect endogenous expression patterns. Thus, it remains to be conclusively determined whether Path or other SLC36 transporters localize to appropriate cellular compartments to function as nutrient sensors for TORC1.

We next set out to characterize Path expression and distribution *in vivo*. To facilitate *in vivo* analysis of SLC36 transporter expression, localization, and dynamic trafficking we used CRISPR-Cas9-mediated genome editing<sup>10,11</sup> to generate a GFP insertion allele (*path*<sup>GFP</sup>) containing the coding sequence for GFP inserted immediately upstream of the stop codon in the last coding exon of *path* (Fig. 1A). Our prior studies demonstrated that addition of GFP to the Path C-terminus does not interfere with the function of *path* transgenes<sup>1</sup>, and we found addition of GFP to the C-terminus of the endogenous locus had no detectable effects on *path* function *in vivo*. First, heterozygosity for *path*<sup>GFP</sup> or placing *path*<sup>GFP</sup> in trans to *path*<sup>dg50</sup> or *Df(3L)BSC773* had no effect on dendrite growth. Further, we noted no obvious differences in developmental timing, body size, or fecundity of *path*<sup>GFP</sup> homozygotes compared to wild type or *path*<sup>GFP/+</sup> controls. We therefore concluded that *path*<sup>GFP</sup> is a functional allele and that we could use *path*<sup>GFP</sup> to monitor endogenous distribution and dynamics of an SLC36 transporter for the first time in a living animal.

For our initial characterization of *path*<sup>GFP</sup> we monitored GFP distribution in well-fed third instar larvae, as the neuronal growth defects we previously described were analyzed in well-fed animals.<sup>1</sup> In third instar larvae, Path<sup>GFP</sup> was broadly expressed (Fig. 3A), consistent with our prior antibody staining results<sup>1</sup>. However, Path<sup>GFP</sup> accumulated to different levels in different tissues, suggesting that Path regulation varies according to tissue type. Within the body wall, Path<sup>GFP</sup> was most highly expressed in epithelial cells, where it accumulated at junctional domains, consistent with plasma membrane localization (Fig. 3B), and sensory neurons, where it was present in axons, cell bodies, and throughout dendrite arbors (Fig. 3B).

Although our phenotypic analysis of *path* mutants has focused on growth control in the PNS, Path<sup>GFP</sup> was expressed at the highest levels in the larval brain and the digestive system. Within the larval brain, Path<sup>GFP</sup> expression was especially high in surface glia (Fig. 3C), suggesting that Path may participate in glial

growth control or nutrient sensing. Notably, a P-element insertion allele of *path* causes increased sensitivity to ethanol-induced sedation and increased ethanol-induced hyperactivity,<sup>16</sup> therefore we speculate that Path may function in glia to modulate these behavioral responses to alcohol in *Drosophila*. Additionally, glial cells form the blood-brain barrier (BBB) in *Drosophila*, providing a barrier to solute diffusion and serving roles in nutrient uptake for the brain,<sup>17</sup> so it will be intriguing to determine whether *path* contributes to BBB function. It should be noted that although there have been no reports on expression or localization of SLC36 at the vertebrate BBB, other members of the  $\beta$  group of SLCs (neutral amino acid transporters) localize to the BBB.<sup>18,19</sup>

Path<sup>GFP</sup> was also present at high levels in the digestive system, thus it seems plausible that Path may function as an intestinal nutrient sensor. Although candidate receptors for carbohydrate sensing in the gut have been identified,<sup>20–22</sup> little is known about the nature of intestinal amino acid sensing programs. Within the digestive system, Path<sup>GFP</sup> was present at the highest levels in the proventriculus (Fig. 3A, D), a structure involved in food maceration as well as insect innate immunity<sup>23</sup>; whether Path functions in processes other than nutrient sensing remains to be determined. In the midgut, Path<sup>GFP</sup> strongly labeled small clusters of cells (arrows, Fig. 3D) that likely correspond to adult midgut progenitor cells (AMPs). AMPs give rise to all of the cells of the adult midgut including intestinal stem cells,<sup>24</sup> therefore it is conceivable that Path functions as a nutrient sensor to regulate proliferation of these precursors.

Finally, we note that Path<sup>GFP</sup> adopted a similar distribution in most cell types: the majority of the protein was predominantly confined to plasma membrane domains (Fig. 3B, E), but low levels of Path<sup>GFP</sup> were present in intracellular puncta (Fig. 3B', E'). Thus, at least in well-fed larvae, negligible amounts of Path appear to localize to lysosomal compartments. Thus, although we cannot rule out a role for Path in TORC1 activation, our results suggest that the connection may be indirect. Notably, some SLC36 transporters can be dynamically trafficked in a nutrient-dependent manner in cultured cells,<sup>6</sup> but similar trafficking patterns have not yet been demonstrated *in vivo*.

### Path regulates translational capacity in non-neuronal tissues

*path* regulates neuron growth by modulating translational output of PNS neurons.<sup>1</sup> Paradoxically, Path is widely expressed but growth defects are manifest specifically in sensory neurons. We therefore wanted to test the hypothesis that *path* regulates translational output in sensory neurons but not other cell types. For these studies we focused on larval body wall epidermis for the following reasons: Path is expressed at high levels in these cells and *path* mutation had no significant effect on size of these cells.<sup>1</sup> We expressed a *UAS-Luciferase* reporter specifically in epithelial cells of wild type control or *path* mutant larvae and measured protein and mRNA expression levels by Luciferase activity assays and qRT-PCR, respectively. To our surprise, *path* mutation caused a significant decrease in epithelial Luciferase activity while causing only a modest decrease in mRNA levels (Fig. 4A), suggesting that *path* regulates translational capacity in epithelial cells as well



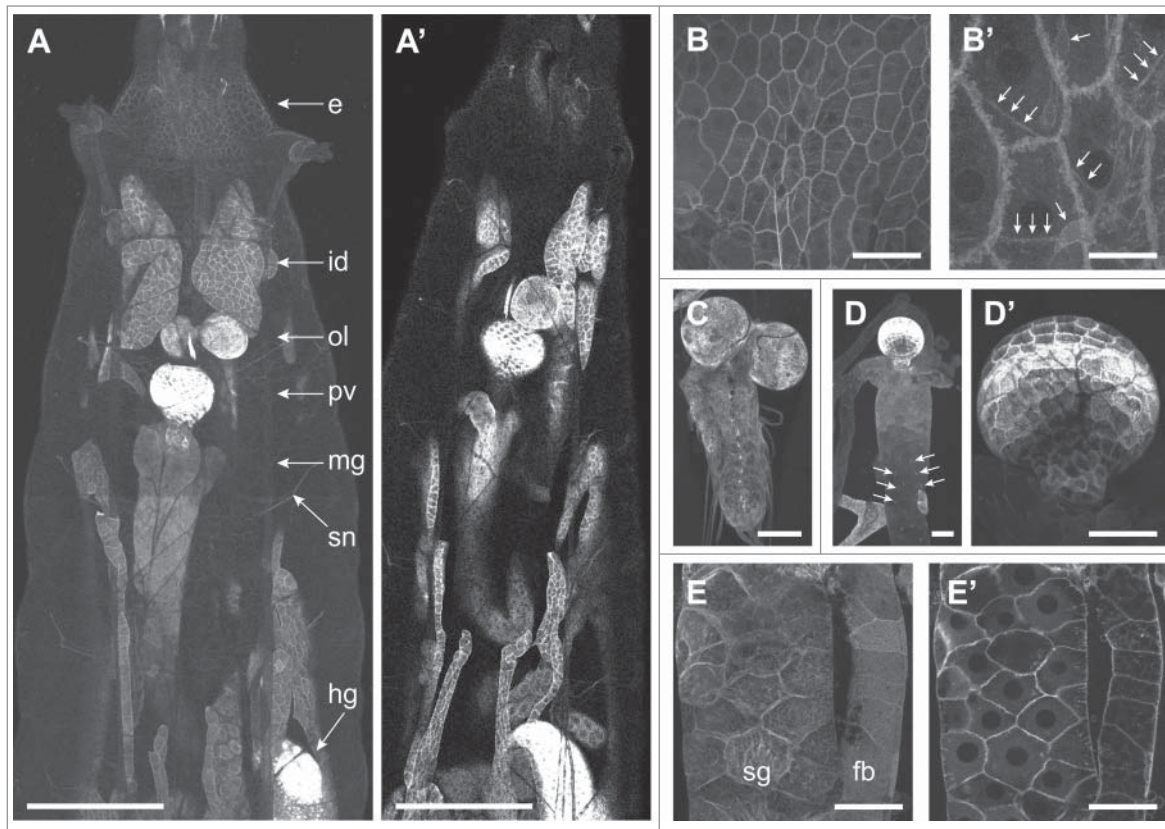


**Figure 3.** Path<sup>GFP</sup> expression in larvae. (A) Path<sup>GFP</sup> is broadly expressed in larvae but present at different levels in different tissues. Abbreviations: e, epidermis; fb, fat body; hg, hindgut; id, imaginal discs; mg, midgut; ol, optic lobe; pv, proventriculus; sg, salivary glands; sn, segmental nerves. Scale bars: 500  $\mu$ m in A, 100  $\mu$ m in all other panels except for B' (25  $\mu$ m). (B) Path<sup>GFP</sup> expression in the body wall, where Path<sup>GFP</sup> accumulates most notably at cell-cell junctions in epithelial cells and is present in cell bodies and dendrites of sensory neurons (B', arrows). Path<sup>GFP</sup> is expressed at high levels in the ventral nerve cord (C), most notably in glia, and in the digestive system (D) where levels are highest in the proventriculus (D'). Arrows in (D) mark cell clusters that likely correspond to adult midgut progenitor cells. Surface (E) and medial (E') cross-sectional views of Path<sup>GFP</sup> expression in a salivary gland and fat body illustrating that Path<sup>GFP</sup> is largely confined to the area of the plasma membrane in most cell types. Genotype: *w<sup>118</sup>; path<sup>GFP</sup>/+*.

as neurons. Although it remains to be determined whether *path* similarly regulates translational output in other cell types, we speculate that Path is broadly utilized to couple nutrient conditions to translational output.

## Discussion

How growth programs are tailored to meet the demands of large neurons is largely unknown. Here, we demonstrate that the SLC36 transporter Path is required for growth of axons and dendrites in large neurons. Although the precise mechanism of action remains to be determined, the amino-terminal intracellular domain is essential for Path function in neuron growth control,<sup>1</sup> and we hypothesize that Path transduces nutrient signals via protein-protein interactions between its N-terminal intracellular domain and unidentified signaling proteins to modulate translational output (Fig. 4B). In light of prior studies suggesting a link between SLC36 transporters and TORC1 signaling<sup>2,6,12</sup> and our observation that co-overexpression of Path and Rheb potentiates dendrite growth,<sup>1</sup> we propose that Path may promote neuron

growth, in part, through regulation of TORC1 activity. However, given our observations that Path primarily localizes to the plasma membrane and that mutations in TORC1 components cause more modest neuron growth deficits than mutation of *path*, it seems likely that Path engages downstream pathways other than TORC1 to promote neuron growth. Although the identity of these pathways is currently unknown, eukaryotic initiation factor 2 (eIF2) activity is regulated by a suite of kinases (eIF2K) that tune translation levels in response to environmental stresses, including amino acid deficiency.<sup>25</sup>

Although Path is broadly expressed, *path* is dispensable for growth in most cell types under well-fed laboratory conditions. One prediction of this observation is that Path selectively affects translation in large neurons. Our results from this study refute this notion; cells that do not require *path* for growth still require *path* for maximum translational output. How can we explain the disparity in growth phenotypes between neurons and other cells? First, Path may play a more significant role in translational control of neurons than other cell types. *Drosophila* has several uncharacterized genes that encode SLC36 transporters, and these gene products may function redundantly to control growth

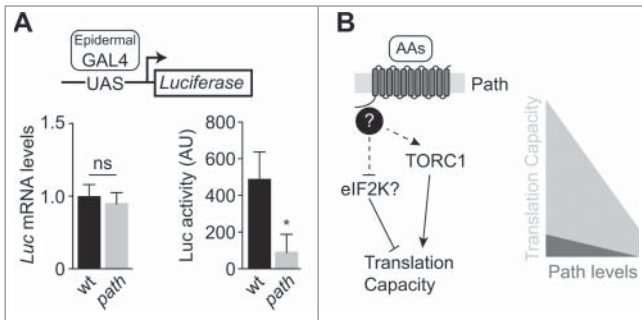


**Figure 4.** *path* regulates translational capacity. **(A)** *path* is required for maximum translational output in non-neuronal cells. *Luciferase* mRNA levels and *Luciferase* activity were assayed in larval body wall extracts of wild type and *path* mutants expressing a *UAS-Rluc-Fluc* bicistronic reporter transgene in epithelial cells (*A58-Gal4*). mRNA levels reflect  $\Delta\Delta Ct$  values for *Luciferase* relative to  $\beta$ -*tubulin* in larval body wall lysates ( $n=6$ ). For *Luciferase* activity, the mean and standard deviation from 6 samples is shown. ns, not significant ( $>0.05P$ ),  $* < 0.05P$ , unpaired t-test with Welch's correction. Genotypes: wt,  $w^{118}; UAS-RLucFluc/+; A58-Gal4/+$ ; *path*,  $w^{118}; UAS-RLucFluc/+; A58-Gal4, path^{dg50}/DF(3L)BSC773$ . **(B)** Putative pathway (left) and model (right) for Path-mediated control of translational capacity. The N-terminal intracellular domain of Path plays a critical role in growth control, perhaps by linking Path to currently unknown signaling molecules (question mark). Some evidence supports a role for TORC1 downstream of Path, but we speculate that additional pathways, possibly including eIF2 kinases, contribute to translational control by Path. Though a baseline level of translation occurs even in the absence of Path protein, Path is required for maximal translational output.

together with Path in some cell types. Consistent with this notion, overexpression of *CG1139*, which encodes another SLC36 transporter, drives ommatidial overgrowth in the eye.<sup>2</sup> Second, the residual translational capacity in *path* mutants is likely sufficient to support normal growth in many cell types, at least under certain conditions. Similarly, loss of *Drosophila* 4E-BP (*Thor*) function reduces overall translation without any obvious effect on animal growth in well-fed conditions.<sup>26</sup> Intriguingly, environmental stresses such as hypoxia or starvation uncover a requirement for *Thor* in growth control. Similarly, we predict that stresses that compromise translational efficiency should sensitize cells to a requirement for *path* function, therefore an exciting future direction will be to determine whether *path* exerts state-dependent functions on growth control.

## Materials and Methods

### Fly stocks

The following alleles were used in this study:  $w^{118}$  (FBal0018157),  $path^{dg50}$  (FBal0305310),  $path^{GFP}$  (this study),  $path^{\Delta}$  (this study), *Df(3L)BSC773* (FBab0045882), *ppk-CD4-tdTomato* (FBti0143432), *ppk.hs-mCD8.3xEGFP* (FBtp0065837), *UAS-Rluc-Fluc* bicistronic reporter (FBtp0108905), *A58-Gal4* (FBti0072310), and *vas-Cas9* (FBti0160473).

### Generation of path alleles

The *path* knockout allele and GFP-tagged *path* knock-in allele were engineered using CRISPR/Cas9 mediated gene editing.<sup>11</sup> Two target sites were selected just outside of the coding region of the shortest isoform, *path-RE*, which includes the four exons shared by all *path* isoforms, using the CRISPR Optimal Target Finder (<http://tools.flycrispr.molbio.wisc.edu/targetFinder/>).<sup>11</sup> chiRNA plasmids were generated by insertion of annealed oligonucleotides into the BbsI site of pU6-BbsI-chiRNA.<sup>10</sup> The donor vector for the *path* knockout allele was cloned by restriction digest, inserting 5' and 3' 1kb homology arms into the NheI and SapI sites, respectively, of the pHD-DsRed plasmid.<sup>14</sup> The donor vector for the *path-GFP* knock-in allele was cloned by Gibson assembly, using the knockout donor vector as a backbone, with GFP fused in-frame with the C-terminal end of *path* and the LoxP-flanked dsRed marker following the GFP stop codon, all internal to the mutated CRISPR target sites. chiRNA and pHD-DsRed plasmids were co-injected into embryos expressing Cas9 in the germline (BL55821:  $y[1] M\{vas-Cas9.RFP\}/ZH-2A w[1118]/FM7a, P\{w[+mC]=Tb[1]\}/FM7-A$ ).

Primers used were as follows:

path chiRNA 1 sense:	cttcgtacacaactgaaactcgcca
path chiRNA 1 antisense:	aaactggcgagtttcagttgtgtac
path chiRNA 2 sense:	cttcgtactcaccatttaggagag
path chiRNA 2 antisense:	aaactctcctaaatggtgaagtac
path homology arm 1 forward:	gccagctagccaaacgaatggaaaagctgtg
path homology arm 1 reverse:	ctcagctagccacggaatcgaagcggttcttatatgctg
path homology arm 2 forward:	gaacgctctcatatgagaggctccgcttcttag
path homology arm 2 reverse:	cgcgctctccgacctctgaatatgtaaatggac
path-GFP backbone forward:	cttcaccacttaggagagagcctccgcttctagataaaatc
path-GFP backbone reverse:	ctgaaactgccacactatcgaagcggttcttatatgctg
path-GFP coding region forward:	ccgcttcgatagtggtggcagtttcagttgtgtacagacg
path-GFP coding region reverse:	cgaagtattctattgtatgttcatccatgccc
path-GFP loxP dsRed forward:	ggcatggatgaactatacaaatagataactcgtataatgtatgc
path-GFP loxP dsRed reverse:	gcgaggctctcctaagtgtgaagtataactcgtatagc

### Live imaging

Larvae were mounted in 90% glycerol under coverslips sealed with grease and imaged on Leica SP5 microscope with a 20x/0.8NA lens (Fig. 2A) or a 40x 1.25NA lens (all other images).

### Luciferase assays

Luciferase assays were as described.<sup>1</sup> Briefly, larvae were lifted in ice cold PBS, lysed in 1x Luciferase Cell Culture Lysis Reagent (Promega), and protein concentrations were measured and normalized. 20  $\mu$ l of cell lysate was analyzed for Renilla luciferase using the Luciferase Assay System (Promega), and

luminescence was measured using a Victor V Plate Reader (Perkin-Elmer). All values were corrected to blank wells and normalized for protein input. For qPCR, RNA was isolated using the RNAqueous Micro kit (Life Technologies), reverse transcribed into cDNA, and transcript levels quantified in SYBR Select (Life Technologies) on an ABI StepOne Plus instrument (Life Technologies). Primers used were Renilla F, GGGTGCTTGTTCGATTC; Renilla R: GGCCATTTCATCCCATGATTC;  $\beta$ -tubulin F, AGACAAGATGGTTCAGGT;  $\beta$ -tubulin R, CGAGGCTCTCTACGATAT. Data was analyzed by the Pfaffl method.<sup>27</sup>

### Measurements

2D projections of Z-stacks were used for computer-assisted dendrite tracing with NeuroLucida (MBF Bioscience), and features were measured using the traces. For these experiments, we imaged control and *path* mutant larvae using identical settings, including the same number and thickness of optical sections.

### Statistical analysis

Differences between group means were analyzed via ANOVA with Tukey's HSD *post hoc* analysis; pairwise comparisons of

group means were done with unpaired t-tests with Welch's correction.

### Disclosure of Potential Conflicts of Interest

No potential conflicts of interest were disclosed.

### Acknowledgments

We thank the Bloomington *Drosophila* Stock Center for fly stocks, Kent Duncan for *UAS-Rluc-Fluc* fly stocks, and Eleanor Lutz for assistance characterizing *path*<sup>GFP</sup> expression.

### Funding

This work was supported by NINDS R01-NS076614, a Klingenstein Fellowship in Neuroscience, a UW Royalty Research Award and a UW Research Innovation award to JZP; and an NSF Graduate Research Fellowship (DGE-1256032) to CRW.

### References

- Lin WY, Williams C, Yan C, Koledachkina T, Luedke K, Dalton J, Bloomsburg S, Morrison N, Duncan KE, Kim CC, et al. The SLC36 transporter Pathetic is required for extreme dendrite growth in *Drosophila* sensory neurons. *Genes Dev* 2015; 29:1120-35; PMID:26063572; <http://dx.doi.org/10.1101/gad.259119.115>
- Goberdhan DCI, Meredith D, Boyd CAR, Wilson C. PAT-related amino acid transporters regulate growth via a novel mechanism that does not require bulk transport of amino acids. *Dev Camb Engl* 2005; 132:2365-75
- Pillai SM, Meredith D. SLC36A4 (hPAT4) is a high affinity amino acid transporter when expressed in *Xenopus laevis* oocytes. *J Biol Chem* 2011; 286:2455-60; PMID:21097500; <http://dx.doi.org/10.1074/jbc.M110.172403>
- Hyde R, Cwiklinski EL, MacAulay K, Taylor PM, Hundal HS. Distinct sensor pathways in the hierarchical control of SNAT2, a putative amino acid transporter, by amino acid availability. *J Biol Chem* 2007; 282:19788-98; PMID:17488712; <http://dx.doi.org/10.1074/jbc.M611520200>
- Stolarczyk E, Guissard C, Michau A, Even PC, Grosfeld A, Serradas P, Lorisignol A, Pénicaud L, Brot-Laroche E, Leturque A, et al. Detection of extracellular glucose by GLUT2 contributes to hypothalamic control of food intake. *Am J Physiol Endocrinol Metab* 2010; 298:E1078-87; PMID:20179244; <http://dx.doi.org/10.1152/ajpendo.00737.2009>
- Ögmundsdóttir MH, Heublein S, Kazi S, Reynolds B, Visvalingam SM, Shaw MK, Goberdhan DCI. Proton-assisted amino acid transporter PAT1 complexes with Rag GTPases and activates TORC1 on late endosomal and lysosomal membranes. *PLoS One* 2012; 7:e36616; <http://dx.doi.org/10.1371/journal.pone.0036616>
- Sancak Y, Bar-Peled L, Zoncu R, Markhard AL, Nada S, Sabatini DM. Regulator-Rag complex targets mTORC1 to the lysosomal surface and is necessary for its activation by amino acids. *Cell* 2010; 141:290-303; PMID:20381137; <http://dx.doi.org/10.1016/j.cell.2010.02.024>
- Rebsamen M, Pochini L, Stasyk T, de Araújo MEG, Galluccio M, Kandasamy RK, Snijder B, Fauster A, Rudashevskaya EL, Bruckner M, et al. SLC38A9 is a component of the lysosomal amino acid sensing machinery that controls mTORC1. *Nature* 2015; 519:477-81; PMID:25561175; <http://dx.doi.org/10.1038/nature14107>
- Zoncu R, Bar-Peled L, Efeyan A, Wang S, Sancak Y, Sabatini DM. mTORC1 senses lysosomal amino acids through an inside-out mechanism that requires the vacuolar H(+)-ATPase. *Science* 2011; 334:678-83; PMID:22053050; <http://dx.doi.org/10.1126/science.1207056>
- Gratz SJ, Cummings AM, Nguyen JN, Hamm DC, Donohue LK, Harrison MM, Wildonger J, O'Connor-Giles KM. Genome engineering of *Drosophila* with the CRISPR RNA-guided Cas9 nuclease. *Genetics* 2013; 194:1029-35; PMID:23709638; <http://dx.doi.org/10.1534/genetics.113.152710>
- Gratz SJ, Ukken FP, Rubinstein CD, Thiede G, Donohue LK, Cummings AM, O'Connor-Giles KM. Highly specific and efficient CRISPR/Cas9-catalyzed homology-directed repair in *Drosophila*. *Genetics* 2014; 196:961-71; PMID:24478335; <http://dx.doi.org/10.1534/genetics.113.160713>
- Heublein S, Kazi S, Ögmundsdóttir MH, Attwood EV, Kala S, Boyd CAR, Wilson C, Goberdhan DCI. Proton-assisted amino-acid transporters are conserved regulators of proliferation and amino-acid-dependent mTORC1 activation. *Oncogene* 2010; 29:4068-79; PMID:20498635; <http://dx.doi.org/10.1038/onc.2010.177>
- Boll M, Daniel H, Gasnier B. The SLC36 family: proton-coupled transporters for the absorption of selected amino acids from extracellular and intracellular proteolysis. *Pflüg Arch Eur J Physiol* 2004; 447:776-9; <http://dx.doi.org/10.1007/s00424-003-1073-4>
- Wreden CC, Johnson J, Tran C, Seal RP, Copenhagen DR, Reimer RJ, Edwards RH. The H<sup>+</sup>-coupled electrogenic lysosomal amino acid transporter LYAAT1 localizes to the axon and plasma membrane of hippocampal neurons. *J Neurosci Off J Soc Neurosci* 2003; 23:1265-75
- Roshanbin S, Hellsten SV, Tafreshiha A, Zhu Y, Raine A, Fredriksson R. PAT4 is abundantly expressed in excitatory and inhibitory neurons as well as epithelial cells. *Brain Res* 2014; 1557:12-25; PMID:24530433; <http://dx.doi.org/10.1016/j.brainres.2014.02.014>
- Devineni AV, McClure KD, Guarnieri DJ, Corl AB, Wolf FW, Eddison M, Heberlein U. The genetic relationships between ethanol preference, acute ethanol sensitivity, and ethanol tolerance in *Drosophila melanogaster*. *Fly (Austin)* 2011; 5:191-9
- Limmer S, Weiler A, Volkenhoff A, Babatz F, Klämbt C. The *Drosophila* blood-brain barrier: development and function of a glial endothelium. *Front Neurosci* 2014; 8:365; PMID:25452710; <http://dx.doi.org/10.3389/fnins.2014.00365>
- Geier EG, Chen EC, Webb A, Papp AC, Yee SW, Sadee W, Giacomini KM. Profiling solute carrier transporters in the human blood-brain barrier. *Clin Pharmacol Ther* 2013; 94:636-9; PMID:24013810; <http://dx.doi.org/10.1038/clpt.2013.175>
- Sundberg BE, Wåag E, Jacobsson JA, Stephansson O, Rumaks J, Svirskis S, Alsö J, Roman E, Ebendal T, Klusa V, et al. The evolutionary history and tissue mapping of amino acid transporters belonging to solute carrier families SLC32, SLC36, and SLC38. *J Mol Neurosci* 2008; 35:179-93; PMID:18418736; <http://dx.doi.org/10.1007/s12031-008-9046-x>
- Miguel-Aliaga I. Nerveless and gutsy: intestinal nutrient sensing from invertebrates to humans. *Semin Cell Dev Biol* 2012; 23:614-20; PMID:22248674; <http://dx.doi.org/10.1016/j.semcdb.2012.01.002>
- Mishra D, Miyamoto T, Rezenom YH, Broussard A, Yavuz A, Slone J, Russell DH, Amrein H. The molecular basis of sugar sensing in *Drosophila* larvae. *Curr Biol* 2013; 23:1466-71; PMID:23850280; <http://dx.doi.org/10.1016/j.cub.2013.06.028>
- Miyamoto T, Slone J, Song X, Amrein H. A fructose receptor functions as a nutrient sensor in the *Drosophila* brain. *Cell* 2012; 151:1113-25; PMID:23178127; <http://dx.doi.org/10.1016/j.cell.2012.10.024>
- Hao Z, Kasumba I, Aksoy S. Proventriculus (cardia) plays a crucial role in immunity in tsetse fly (Diptera: Glossinidae). *Insect Biochem Mol Biol* 2003; 33:1155-64; PMID:14563366; <http://dx.doi.org/10.1016/j.ibmb.2003.07.001>
- Jiang H, Edgar BA. Intestinal stem cells in the adult *Drosophila* midgut. *Exp Cell Res* 2011; 317:2780-8; PMID:21856297; <http://dx.doi.org/10.1016/j.yexcr.2011.07.020>

25. Wek RC, Jiang HY, Anthony TG. Coping with stress: eIF2 kinases and translational control. *Biochem Soc Trans* 2006; 34:7-11; PMID:16246168; <http://dx.doi.org/10.1042/BST0340007>
26. Teleman AA, Chen YW, Cohen SM. 4E-BP functions as a metabolic brake used under stress conditions but not during normal growth. *Genes Dev* 2005; 19:1844-8; PMID:16103212; <http://dx.doi.org/10.1101/gad.341505>
27. Pfaffl MW. A new mathematical model for relative quantification in real-time RT-PCR. *Nucleic Acids Res* 2001;29:e45